CRYSTAL GROWTH & DESIGN
2008
VOL. 8, NO. 9
3144–3147

Single Crystalline Semi-Nanotubes of Indium Germanate

Chaoyi Yan, Tao Zhang, and Pooi See Lee*

School of Materials Science and Engineering, Nanyang Technological University, Singapore 639798

Received May 10, 2008; Revised Manuscript Received July 17, 2008

ABSTRACT: Single crystalline $In_2Ge_2O_7$ nanotubes were synthesized by a thermal evaporation method. The growth mechanism of those novel seminanotubular structures was explained to be a vapor−liquid−solid (VLS) mechanism. Its morphology and structures were studied by X-ray diffraction (XRD), scanning electron microscopy (SEM), transmission electron microscopy (TEM), and energy dispersive spectroscopy (EDS). The semi-nanotubes have widths of 80−500 nm and lengths of 5−20 μm. As-synthesized products were found to be single crystalline $In_2Ge_2O_7$ with a monoclinic crystal structure. Indium particles serve as catalysts to direct nanotube growth. Germanium concentration nonuniformity is proposed to be the reason for a semi-nanotubular structure nucleation rather than nanotubes or nanowires.

Nanoscale one-dimensional (1D) structures, such as nanowires, nanobelts, and nanotubes, are of particular interest due to their unique properties and potential applications superior to their bulk counterparts.[1−3] However, compared with the fabrication processes of 1D nanowires, the synthesis of nanotubes are relatively more complex and difficult due to the characteristic hollow structures. Therefore, many recent research efforts have been dedicated to the large-scale and facile syntheses of nanotubes.

Apart from synthesis of nanotubes based on binary compounds with a layered structure,[4−8] templates such as nanoporous alumina, carbon nanotubes, and removable nanowires have been utilized to fabricate predominantly amorphous or polycrystalline nanotubes.[9,10] Large-scale synthesis of single crystalline nanotubes can be realized by epitaxial casting[11] or solid-state interdiffusion based on the Kirkendall effect,[12] although they are only applicable to specific groups of materials. Nanoscale tubular structures would be advantageous in potential high-efficiency catalysis, capillarity or biochemical-sensing applications.

Germanates have attracted attention in the areas of catalysis, adsorption, ion exchange, porous materials for humidity sensors and germanate glass as a window for high energy laser systems.[13−16] 1D indium germanate ($In_2Ge_2O_7$) nanostructures have rarely been studied except for two reports about the synthesis of microtubes and nanobelts via a vapor−solid (VS) mechanism.[17,18] In this paper, we report the successful synthesis of single crystalline $In_2Ge_2O_7$ semi-nanotubes grown via a self-catalyzed vapor−liquid−solid (VLS) mechanism. We present a thorough analysis of their morphological and structural characteristics as well as the growth process. This peculiar semitubular structure may find its applications as the intermediate morphology between nanobelts and nanotubes.

The experimental apparatus consists of a horizontal quartz tube placed inside a tube furnace. Ge powder (99.999%, Alfa Aesar), In_2O_3 powder (99.999%, Strem Chemicals), and activated carbon powder (>99%, Sigma Aldrich) with an atomic ratio of about 2:1:3 placed in a quartz crucible was used as solid source and mounted in the middle of the high-temperature zone. A cleaned p-type Si (100) wafer was placed 15−20 cm from the powder source at a growth temperature of 300−400 °C. The temperature of the furnace was increased to 1000 °C at a rate of 10 °C min^{-1} and kept at that temperature for 30 min under a constant argon flow of 90 sccm (standard cubic centimeter per minute). Ambient pressure inside the tube was around 1 Torr during the entire process. Subsequently, the furnace was cooled to room temperature.

A typical low magnification scanning electron microscopy (SEM) image (cross-section view) of the products is shown in Figure 1a. The products are composed of a large quantity of 1D nanostructures

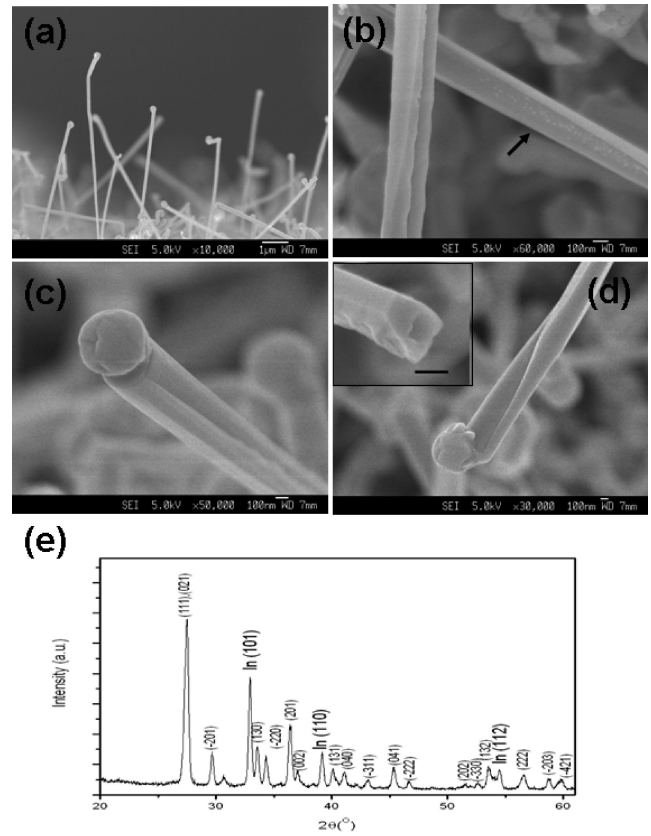

Figure 1. SEM images of $In_2Ge_2O_7$ seminanotubes. (a) Low magnification of cross-section view; (b−d) high-magnification of the nanotubes revealing the semitubular structure and catalyst particles at the front. Inset in (d) shows an open end of a single nanotube. Scale bar is 100 nm; (e) XRD pattern of the products.

with diameters and lengths in the range of 80−500 nm (corresponds to the catalyst particle sizes) and 5−20 μm, respectively. High magnification SEM images reveal that those structures are semi-nanotubes with hemispherical catalyst particles at the front. Representative magnified images of the body and tip of semi-nanotubes are shown in Figure 1b−d. Cross-sections of the semi-nanotubes are polygonous (Figure 1c), and a typical one with a roughly rectangular cross-section is shown in the inset of Figure 1d. X-ray diffraction (XRD) pattern of the product is shown in Figure 1e. The spectrum suggests two crystalline phases, that is, monoclinic $In_2Ge_2O_7$ (JCPDS card 26-0768: a = 6.658 Å, b =

* Corresponding author. Phone: (65)-67906661; fax: (65)-67909081; e-mail: pslee@ntu.edu.sg. Web: http://www.ntu.edu.sg/home/pslee/.

10.1021/cg8004882 CCC: $40.75
Published on Web 08/12/2008

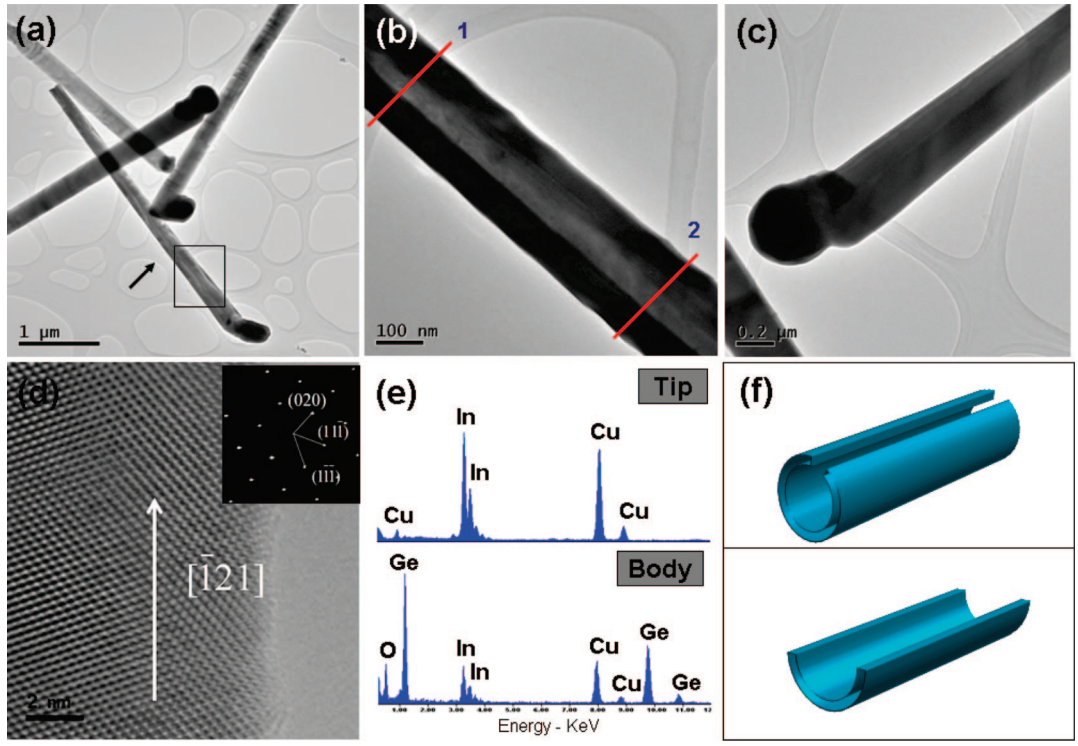

Figure 2. (a) Low magnification TEM image of the $In_2Ge_2O_7$ semi-nanotubes; (b,c) magnified TEM images of the body and tip of a single nanotube; (d) HRTEM image, inset is the corresponding SAED pattern recorded along the [101] zone axis; (e) EDS spectra taken from the tip and body of a nanotube; (f) schematic illustrations of the semitubular structures for those shown in (b) more than a half and (c) less than a half, respectively.

8.784 Å, c = 4.9266 Å, β = 102.48°) and tetragonal In (JCPDS card 5−0642: a = 3.2517 Å, c = 4.9459 Å).

More detailed structure and composition analysis of the products were carried out by transmission electron microscopy (TEM), high resolution TEM (HRTEM), selected area electron diffraction (SAED) pattern, and energy dispersive spectroscopy (EDS). Figure 2a shows a typical low magnification TEM image of the $In_2Ge_2O_7$ nanotubes. Higher magnification images of the body and tip are shown in Figure 2, panels b and c, respectively. A hemispherical tip can be clearly observed at the front, and instead of a complete cylinder tubular structure, the tube wall in Figure 2c consists of almost half of a circle, revealing the peculiar semi-nanotube structure.

The nanotubes are frequently observed to be tapered as shown in Figure 1b, Figure 2a (indicated by black arrows), and Figure 2b. In contrary to conventional tapering of nanowires, that is, the diameter of the nanowires decreases from bottom to top due to uncatalyzed decomposition of growth precursors[19] or catalyst migration,[20] diameters of the nanotubes here increase as they grow. Diameters of the tube segment shown in Figure 2b increase from 180 nm (position 1) to 219 nm (position 2). One reason is that the tube walls are rolling up as the growth proceeds (Figure 1b,d), and subsequently the freshly grown parts of the nanotubes possess larger diameters than those segments away from the tips. In Figure 2b the opening widths (light region) of position 1 and 2 are 67 and 104 nm, respectively. But it is worth noticing that instead of the real width of the inner cavity, the width of the light region is the opening between adjacent tube-walls, due to the incomplete tubular structure. Another possible reason is that the volumes of the liquid droplets grow larger as a result of continuous and simultaneous adsorption of In and Ge species from vapor phase.

A typical HRTEM image is shown in Figure 2d. The SAED pattern (Figure 2d inset) is recorded along the [101] zone axis of a monoclinic $In_2Ge_2O_7$ crystal. Growth direction of the nanotube is found to be parallel to [$\bar{1}$21]. All other $In_2Ge_2O_7$ semi-nanotubes were also confirmed to be single crystalline, although a different growth direction, such as [1$\bar{1}$1], was observed (Figure S1, Supporting Information). EDS spectra taken from the tip and body of the semi-nanotubes are shown in Figure 2e. They confirm that the tip is composed of indium, while the body is composed of indium, germanium, and oxygen with an indium to germanium atomic ratio of roughly 1:1. Figure 2f are two schematic illustrations of the semitubular structures for images shown in Figure 2b (up one, more than a half) and Figure 2c (bottom one, less than a half), respectively. The catalyst tips are omitted for clarity.

The growth of those single crystalline $In_2Ge_2O_7$ seminanotubes can be explained by a VLS mechanism, which is first proposed by Wagner and Ellis to explain the metal-catalyzed whisker growth in micrometer scale.[21] According to this mechanism, a small catalyst particle forms eutectic liquid alloy with the host material at the growth temperature. The liquid droplet is readily supersaturated with reaction species supplied from the surrounding vapor. Precipitation of supersaturated species at the solid−liquid interface leads to 1D nanostructure growth.[21]

The growth process here is self-catalyzed where indium serves as catalyst for $In_2Ge_2O_7$ nanotube growth. In, In_2O, and Ge vapor from the high temperature region would condense and form liquid droplets on the substrates when they were brought to the low temperature region by Ar flow. Continuous adsorption of those vapor species led to the precipitation of $In_2Ge_2O_7$ at the solid−liquid interface when combined with residual oxygen in the furnace. Instead of the precipitation of pure Ge which leads to the growth of Ge nanowires,[22] formation of $In_2Ge_2O_7$ compound results from the simultaneous adsorption of both In and Ge species from the vapor phase.

During the cooling process when no more vapor species were available, residual Ge in the liquid alloy would continue to precipitate until exhausted, leaving In tips with Ge content below the detection level. This is consistent with the Ge−In binary alloy phase diagram[23] as shown in Figure 3a (small amount of oxygen is not expected to change the diagram significantly). A higher In concentration is required if the binary alloy wants to solidify at a lower temperature. And this indium ratio reaches almost 100% when the products are cooled to a temperature below 158 °C. Although

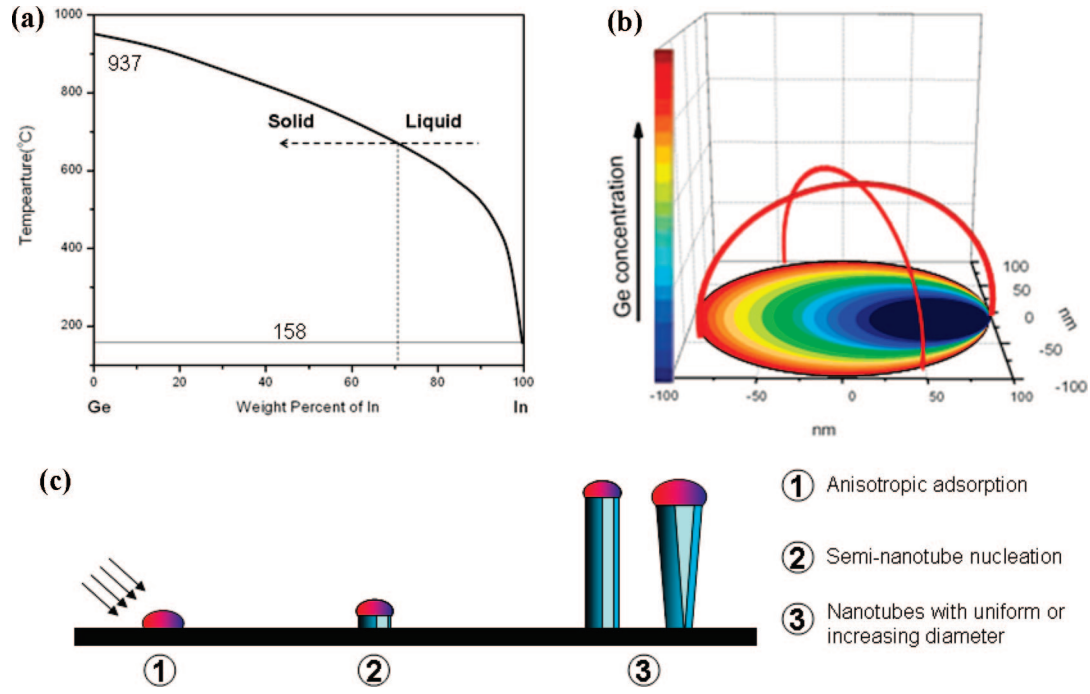

Figure 3. (a) Binary phase diagram of Ge−In, showing that a higher In concentration is required if the liquid alloy were to solidify at a lower temperature; (b) germanium concentration gradient at the liquid−substrate interface (a circle with a diameter of 200 nm). The cap of the liquid droplet is omitted for clarity; (c) schematic illustration of the seminanotube nucleation and growth processes.

it is possible that the liquid droplet may contain oxygen during the growth process due to the generation of In_2O[17] from carbon-thermal reduction of In_2O_3, it is not a stable compound and would decompose during the cooling process, forming $In_2Ge_2O_7$—a much more stable ternary oxide of indium and germanium at ambient pressure.[17,24] This is verified by the fact that tetragonal In peaks were detected in XRD measurements and EDS spectrum reveals the catalyst tips contain only indium while germanium and oxygen contents are below detection level after growth.

One important issue to be addressed is why seminanotubes are nucleated rather than complete nanotubes or nanowires. We suggest that germanium concentration gradient near the liquid−substrate interface may play the key role during the nucleation stage. Simulation results of a three-dimensional growth model[25] for Au-catalyzed GaAs nanowire with a diameter of 60 nm reveal that the gallium concentration at the edges of the liquid−solid interface is higher than that at the center due to a much shorter gallium diffusion distance. And the authors predicted the possibility for formation of tubular-shaped nanowires based on this concentration gradient.[25] Although the simulation result is based on solid-phase diffusion, this is also the case for catalyst particles in the liquid state during growth.[26] The average diameter of the $In_2Ge_2O_7$ nanotubes here is around 300 nm. Those relatively large diameters would make it more difficult for germanium to distribute uniformly through the whole liquid−substrate interface and exacerbate the concentration variation, with the edges having a higher concentration than the central regions. Concentration variation along the edge may be attributed to the shadowing effect originating from anisotropic vapor adsorption as well as the exacerbated concentration variation. As a result, part of the edge possesses the highest germanium concentration as shown in Figure 3b. Places with high concentration would reach supersaturation first and turn to be nucleation sites for continuous nanotube growth. A schematic illustration of the seminanotube nucleation and growth process is shown in Figure 3c. It is suggested that germanium concentration gradient either through the liquid−substrate interface or along the edges may account for the nucleation of the semi-nanotubular structure, although more work is needed to clarify this relationship.

In summary, we have successfully synthesized large-scale $In_2Ge_2O_7$ semi-nanotubes by a thermal evaporation method. The growth mechanism is a self-catalyzed VLS process where indium serves as a catalyst to direct the nanotube growth. The semi-nanotubes are usually tapered with increasing diameter either due to the tube-wall rolling up or a volume increase of the liquid droplets. Although the liquid droplet may contain germanium or oxygen during growth, they tend to be precipitated when the furnace is cooled, since a higher indium concentration is required at a lower solidification temperature according to the liquidus line of Ge−In alloy. The nucleation of semi-nanotubes, instead of nanowires or nanotubes, is a result of Ge concentration nonuniformity considering the relatively large diameters of the liquid droplets.

Acknowledgment. The authors thank Y. Setiawan, M. Y. Chan, and J. M. Wang for their insightful discussions. We also acknowledge S. S. Pramana and J. Guo for their technical support.

Supporting Information Available: HRTEM image and FFT pattern of the indium germanate semi-nanotubes growing along the [1$\bar{1}\bar{1}$] direction. This material is available free of charge via the Internet at http://pubs.acs.org.

References

(1) Iijima, S. *Nature* **1991**, *354*, 56.
(2) Cui, Y.; Wei, Q.; Park, H.; Lieber, C. M. *Science* **2001**, *293*, 1289.
(3) Xia, Y.; Yang, P.; Sun, Y. *Adv. Mater.* **2003**, *15*, 353.
(4) Suenaga, K.; Colliex, C.; Demoncy, N.; Loiseau, A.; Pascard, H.; Willaime, F. *Science* **1997**, *278*, 653.
(5) Kang, H. P.; Jaewon, C.; Hae, J. K.; Jin, B. L.; Seung, U. S. *Chem. Mater.* **2007**, *19*, 3861.
(6) Macak, J. M.; Tsuchiya, H.; Schmuki, P. *Angew. Chem., Int. Ed.* **2005**, *44*, 2100.
(7) Zhu, Y. Q.; Sekine, T.; Brigatti, K. S.; Firth, S.; Tenne, R.; Rosentsveig, R.; Kroto, H. W.; Walton, D. R. *J. Am. Chem. Soc.* **2003**, *125*, 1329.
(8) Golberg, D.; Bando, Y.; Tang, C. C.; Zhi, C. Y. *Adv. Mater.* **2007**, *19*, 2413.
(9) Ajayan, P. M.; Stephan, O.; Redlich, P.; Colliex, C. *Nature* **1995**, *375*, 564.
(10) Martin, C. R. *Science* **1994**, *266*, 1961.

(11) Goldberger, J.; He, R.; Zhang, Y.; Lee, S.; Yan, H.; Choi, H.; Yang, P. *Nature* **2003**, *422*, 599.
(12) Knez, H.; Scholz, R.; Nielsch, K.; Pippel, E.; Hesse, D.; Zacharias, M.; Gosele, U. *Nat. Mater.* **2006**, *5*, 627.
(13) Gier, T. E.; Bu, X.; Feng, P.; Stucky, G. D. *Nature* **1998**, *395*, 154.
(14) Liu, G.; Zheng, S; Yang, G. *Angew. Chem., Int. Ed.* **2007**, *46*, 2827.
(15) Hogan, M. J.; Brinkman, A. W.; Hashemi, T. *Appl. Phys. Lett.* **1998**, *72*, 3077.
(16) Bayya, S. S.; Chin, G. D.; Sanghera, J. S.; Aggarwal, I. D. *Opt. Express* **2006**, *14*, 11687.
(17) Zhan, J.; Bando, Y.; Hu, J.; Yin, L.; Yuan, X.; Sekiguchi, T.; Golberg, D. *Angew. Chem., Int. Ed.* **2006**, *45*, 228.
(18) Su, Y.; Li, S.; Xu, L.; Chen, Y.; Zhou, Q.; Peng, B.; Yin, S.; Meng, X.; Liang, X.; Feng, Y. *Nanotechnol.* **2006**, *17*, 6007.
(19) Adhikari, H.; Marshall, A. F.; Chidsey, C. E.; McIntyre, P. C. *Nano. Lett.* **2006**, *6*, 318.
(20) Hannon, J. B.; Kodambaka, S; Ross, F. M.; Tromp, R. M. *Nature* **2006**, *440*, 69.
(21) Wagner, R. S.; Ellis, W. C. *Appl. Phys. Lett.* **1964**, *4*, 89.
(22) Sun, X.; Calebotta, G.; Yu, B.; Selvaduray, G.; Meyyappan, M. *J. Vac. Sci. Technol. B.* **2007**, *25*, 415.
(23) Massalski, T. B., Ed. *Binary Alloy Phase Diagrams*, 1st ed.; ASM International: Materials Park, OH, 1986.
(24) Shannon, R. D.; Sleight, A. W. *Inorg. Chem.* **1968**, *7*, 1649.
(25) Persson, A. I.; Larsson, M. W.; Sternstrom, S.; Ohlsson, B. J.; Samuelson, L.; Wallenberg, L. R. *Nat. Mater.* **2004**, *3*, 677.
(26) Bakkers, E.; Verheijen, M. A. *J. Am. Chem. Soc.* **2003**, *125*, 3440.

CG8004882